Figure 3 of a paper by Philippe A. Pezard and Roger N. Anderson, entitled "Morphology and Alteration of the Upper Oceanic Crust from *In-Situ* Electrical Experiments in DSDP/ODP Hole 504B," was printed incorrectly. This figure is on page 136 of SR Vol. 111. Page 136, with the correct Figure 3, is reproduced below in its entirety.

On the following two pages, pages 137 and 139 from this same paper are reprinted with corrections.

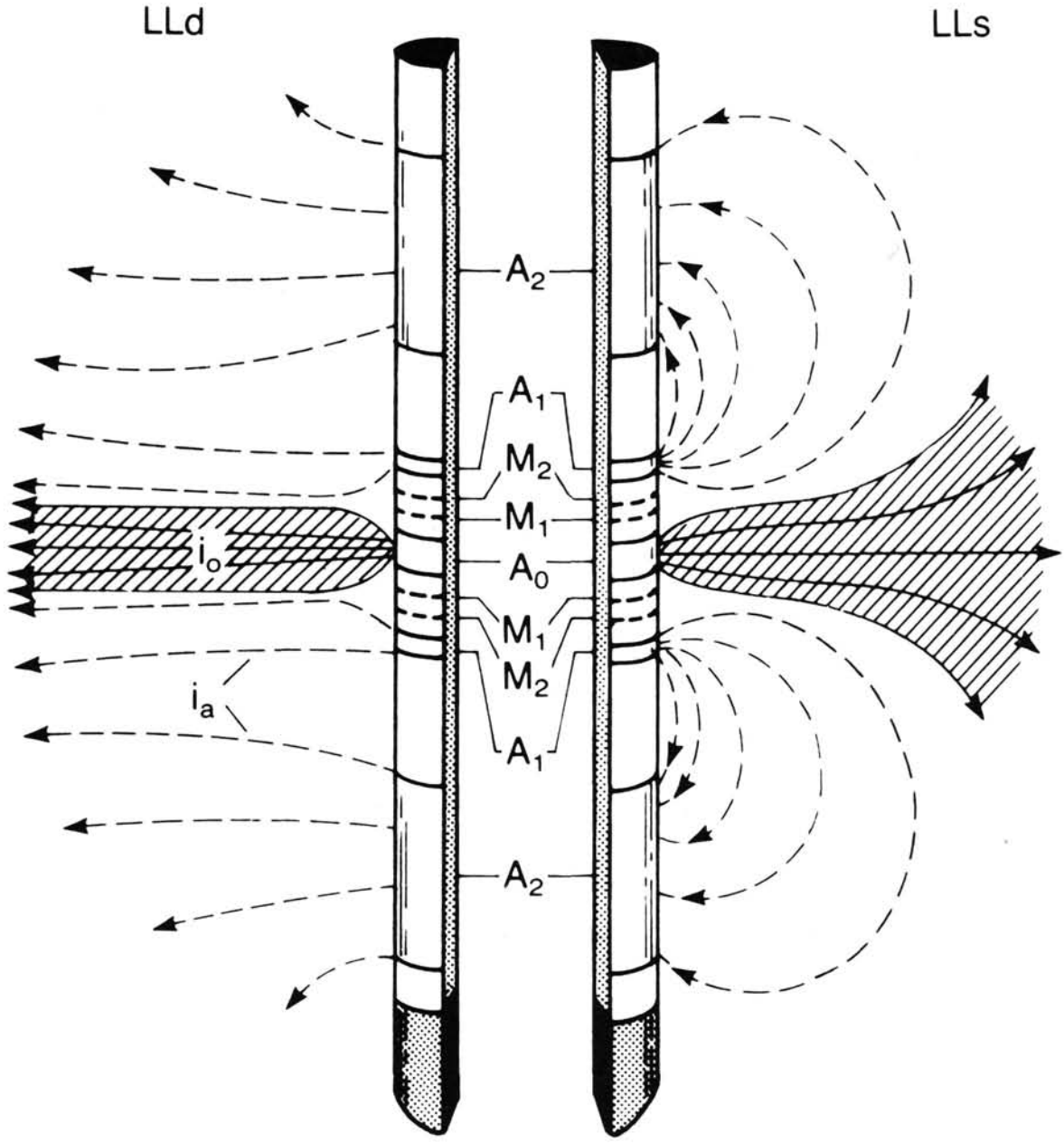

Figure 3. Sketch of the dual laterolog sonde (DLL) and idealized current flow into the rock, with the "shallow" current (*LLs*) to the right and the "deep" current (*LLd*) to the left. The electrode arrangement is labeled in the middle of the split sonde.

When the porosity structure of a hydrocarbon reservoir is being analyzed, a large resistivity contrast is present between waters located in and around the borehole (usually saline and conductive) and hydrocarbons located in the reservoir. In the case of the upper oceanic crust drilled with seawater, borehole and pore fluids have similar salinities (Mottl et al., 1983), and the invasion of the fractures by a fluid of a different salinity than that of seawater can be ignored. The difference between LLs_c and LLd_c is then attributed solely to an anisotropic distribution of the pore space in the rock. In addition, the fact that drilling-related fractures do not extend more than a few decimeters away from the borehole (Kirsch, 1898), far less than the rock volume investigated with the DLL, suggests that they contribute little to the overall signal.

The sketch of two extreme types of fractured rocks in Figure 4 shows that subhorizontal conductive fractures are seen in parallel with the basaltic matrix for the deep measurement, which consequently reduces the value of *LLd* more than that of *LLs*

The equations on page 137 of SR Vol. 111 were given incorrectly. Page 137 is reproduced below in its entirety with the corrected equations shown.

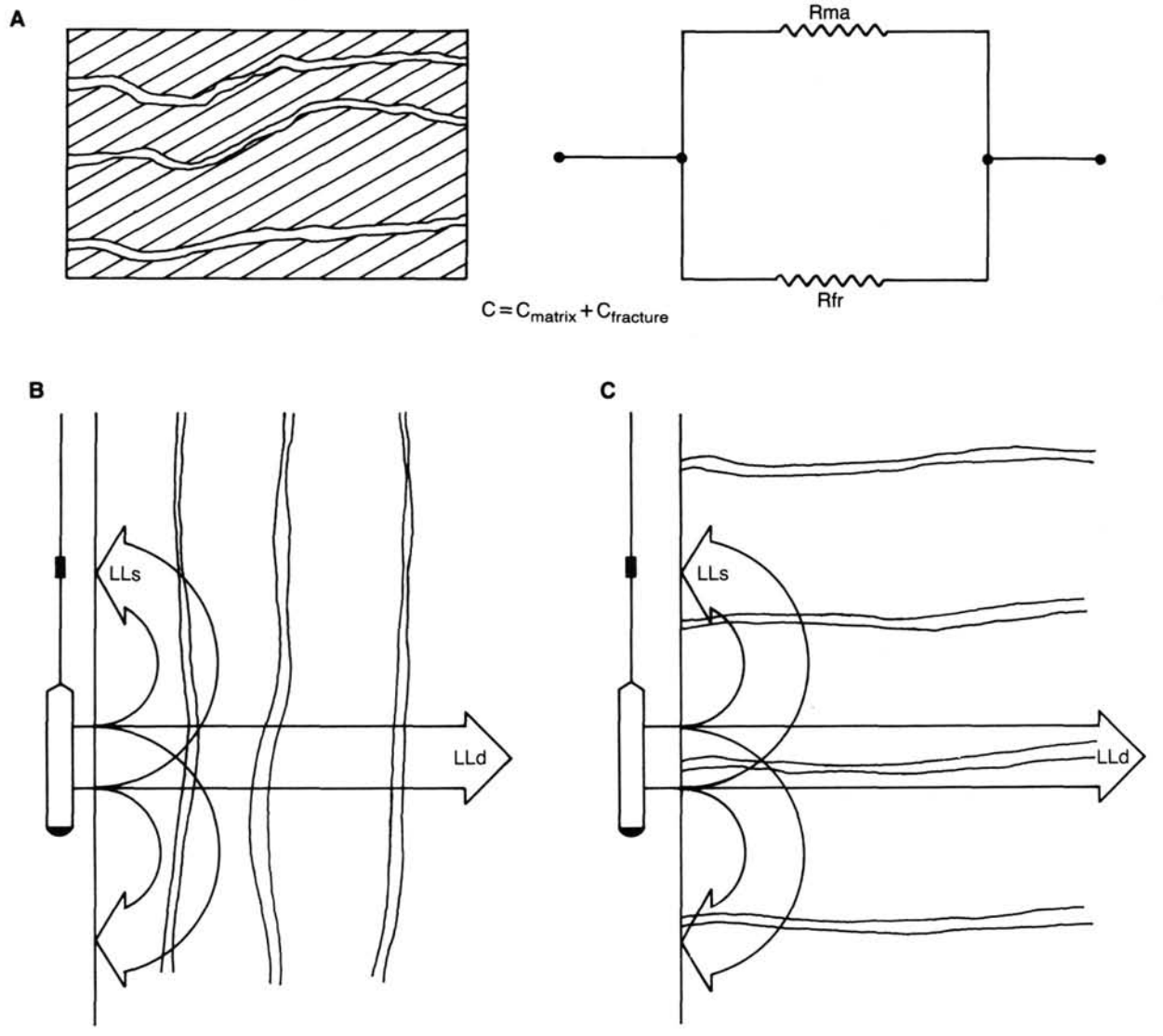

Figure 4. **A**. Resistivity model for matrix and fractures seen by the laterolog measuring currents, with an analogy to electrical circuits in parallel. C = conductivity; Rma = matrix resistivity; Rfr = fracture resistivity. **B**. Idealized vertical fracture network. **C**. Idealized horizontal fracture network.

($LLd < LLs$). In the case of a subvertical network, the relationship is reversed ($LLs < LLd$), and the equation derived by Boyeldieu and Winchester (1982) can be rewritten as

$$\text{VFRPHI} > \text{VFRPHI(min)} = [(1/LLs_c - 1/LLd_c)/(1/R_w)]^{1/mf},$$

where VFRPHI is the "subvertical" fracture porosity, VFRPHI(min) the estimate for vertical fracture porosity, and mf the exponent in Archie's formula for the fracture network. As an estimate of fracture porosity, this computation defines only a lower limit because the presence of any horizontal fractures decreases LLd_c significantly, which consequently tends to reduce the estimate for vertical fracture porosity VFRPHI(min). Similarly, a subhorizontal distribution of fractures would give

$$\text{HFRPHI} > \text{HFRPHI(min)} = [(1/LLd_c - 1/LLs_c)/(1/R_w)]^{1/mf},$$

where HFRPHI is the "subhorizontal" fracture porosity and HFRPHI(min) the estimate for horizontal fracture porosity. These two estimates of fracture porosity are plotted in Figure 5B. The remaining area between fracture porosity (computed as VFRPHI(min) + HFRPHI(min); Fig. 5B) and total porosity (ϕ) is therefore a measurement of residual porosity. This residual is supposed to equate to intergranular pore space, as no vesicular pore space was observed in the cores for these tholeiitic submarine basalts.

One of the main shortcomings related to the use of constant parameters for Archie's formula over the entire length of the drill hole (here $a = 1.0$ and $m = 2.0$), however, is that the variations of rock type, pore space distribution, or alteration facies are not accounted for. Particularly, the presence of conductive clay minerals, such as smectites and chlorites, should be considered in order to avoid misinterpreting them as pore space. In order to account for this, the surface conduction associated with the presence of clays was first mentioned as playing an important role in decreasing the electrical resistivity of sedimentary

The last two equations on page 139 of SR Vol. 111 were given incorrectly. Page 139 is reproduced below in its entirety with the corrected equations shown.

rocks by Winsauer and McCardell (1953), and then Hill and Milburn (1956), and associated to an electrical circuit located in parallel to the pore space (Waxman and Smits, 1968) with

$$FF'' = (C_w + BQ_v)/CLLd_c,$$

where

FF'' = formation factor of the rock corrected for clay conductivity,
C_w = conductivity of the pore fluid,
B = equivalent conductance of the sodium ions absorbed onto the clays,
Q_v = cation exchange capacity of the rock normalized to unit pore volume,
$CLLd_c$ = conductivity of the fluid-bearing rock measured by the deep laterolog.

Rink and Schopper (1974) and Clavier et al. (1977) developed more sophisticated models (reviewed in Pape and Worthington, 1983; Serra, 1984; Ellis, 1987). These models refer as well to the analogy of resistors in parallel used by Waxman and Smits (1968) to describe the conductance of clay-bearing rocks. In order to account for the presence of clays, these authors emphasize the need to determine the intrinsic formation factor of each analyzed core sample, with measurements made using different fluid salinities, rather than the apparent formation factor (*FF*) obtained from one point only (see, in particular, Worthington, 1985). Here again, the behavior of the rock-clay-fluid assemblage at low-fluid conductivity depends considerably on the pore space distribution. For example, Clavier et al. (1977) showed that the apparent formation factor decreases to values near zero at low resistivity for shaly sands, whereas Pape et al. (1985) found that it rises to infinity in slightly altered granites (in fact, $1/FF$ goes to zero). In both cases, they concluded that conduction at low fluid salinity is primarily due to the interlayer conductivity of the clays. Such opposite behavior stresses the need to consider each assembly age individually in order to be able to study the appropriate small-scale conduction mechanism.

In the case of basaltic rocks, the influence of clay conductivity on resistivity was studied and discussed by Drury and Hyndman (1979), Olhoeft (1981), and Karato (1985). In particular, Olhoeft (1981) showed that surface conduction of clays, usually negligible at low temperature, becomes as important as pore conduction at about 80°C and predominant at higher temperatures. This temperature dependence might then play an important role in controlling the resistivity of *in-situ* measurements in deep, hot boreholes such as Hole 504B. The derivation of a more accurate resistivity-porosity transform seems therefore related first to a precise estimation of the conducting clay fraction and second to the study of the temperature dependence of conduction on clay surfaces.

The cation exchange capacity (CEC) is used to characterize the ability of a clay-rich rock sample to absorb electrolytic cations onto pore surfaces, hence creating an additional path for current conduction in parallel to the pore space. The CEC of a rock sample is related to the mobility of the cations (which is equivalent to the adsorption capacity of the clay mineral for a given type of cation), the charge density per unit area, and the specific surface area of the clays distributed on pore surfaces. However, the CEC of rocks cannot be directly and continuously measured at present in a borehole. Measurements of CEC are therefore limited to either *in-situ* complex resistivity experiments or chemical analysis in the laboratory. Such difficulty has consequently required the reconstruction of synthetic CEC profiles from other continuous measurements, on the basis of the calibration points obtained in the laboratory. In particular, the recent development of geochemical logging has provided a way to extract petrophysical parameters such as the CEC from the derived mineralogy (Herron, 1986). Assuming that the relative proportions of each clay mineral of known CEC is provided from the mineralogy derived from the geochemical log, an estimate of the CEC of the rock assemblage can be computed using a linear summation.

The mineralogical inversion of the geochemical data recorded in Hole 504B during Leg 111 is discussed in detail by Anderson et al. (this volume), and the results are presented in Figure 5C. The elemental composition was solved for the presence of smectite (50 meq/100 g) and chlorite (10 meq/100 g) and then used as input to obtain the reconstructed CEC curve (Fig. 5D). In addition, a total of 61 samples selected from Hole 504B was analyzed in the laboratory and measured for CEC (Pezard et al., this volume). In the cores, the quasiuniform presence of smectites as an alteration phase of olivine is reflected by high values of CEC in the extrusive part of the crust (Fig. 6). In the massive flows of Layers 2A and 2B, the average CEC is high (5.8 meq/100 g). Because low initial porosity constrains a low permeability and, in turn, a low water/rock ratio during hydrothermal circulation, a small amount of alteration might be expected from the low average porosity (1.4%) and the absence of fractures in most of these samples selected from massive units. To the contrary, the more porous and fractured pillows have an average CEC value of 10.2 meq/100 g (Pezard et al., this volume). In the massive units of Layer 2C where greenschist facies of alteration are observed, the average CEC value decreases to 2.3 meq/100 g. The CEC laboratory measurements and the reconstructed CEC profile plotted for comparison in Figure 5D are in excellent agreement throughout the hole, although more measurements in the extremely altered upper part of the basement would be desirable.

A new estimate of porosity (ϕ_c) was consequently computed from the equation of Waxman and Smits (1968) and the conservative approach followed by Becker (1985), in which a and m are set to 1.0 and 2.0, respectively:

$$\phi_c^2 = CLLd_c/(C_w + BQ_v),$$

where B reflects the sodium charge mobility and is estimated from Serra (1984) as

$$B = (4.6) \cdot [(1.0) - (0.6) \cdot \exp(-0.077/R_w)],$$

and Q_v is the CEC normalized to unit pore volume, obtained from

$$Q_v = \mathrm{CEC} \cdot \rho \cdot [(1 - \phi)/\phi],$$

with ρ representing the bulk density of the material.

As porosity (ϕ_c) is the estimated parameter, an initial guess for porosity (ϕ) was necessary as an input to the previous equation in order to start to iterate toward a solution constrained by core measurements. The initial value of porosity (ϕ) obtained from Archie's formula was subsequently used to normalize Q_v and, therefore, estimate ϕ_c. Whereas the estimate of porosity (ϕ) derived from Archie's formula proposes relatively high values of total porosity (Fig. 5E), the clay-corrected estimate (ϕ_c) obtained after the first iteration reduces the previous estimate by half in Layers 2A and 2B and to almost zero in the transition zone and the dikes of Layer 2C. This first clay-corrected estimate (shaded green Fig. 5E) appears to be in good agreement with the core measurements throughout the hole. Such an agreement would be expected if the samples analyzed in the laboratory were fully representative of *in-situ* physical properties. Unfortunately, large-scale features such as cracks and voids, for ex-